Available online at www.sciencedirect.com
SCIENCE DIRECT®
Journal of Power Sources 146 (2005) 213–216
JOURNAL OF POWER SOURCES
www.elsevier.com/locate/jpowsour

Comparative study of $Li[CrTi]O_4$, $Li[Li_{1/3}Ti_{5/3}]O_4$ and $Li_{1/2}Fe_{1/2}[Li_{1/2}Fe_{1/2}Ti]O_4$ in non-aqueous lithium cells

Kazuhiko Mukai [a,b], Kingo Ariyoshi [b], Tsutomu Ohzuku [b,*]

[a] *TOYOTA Central R&D Labs., Inc. (TCRDL), Aichi 480-1192, Japan*
[b] *Department of Applied Chemistry, Graduate School of Engineering, Osaka City University (OCU), Sugimoto 3-3-138, Osaka 558-8585, Japan*

Available online 27 April 2005

Abstract

Comparative study of $Li[CrTi]O_4$, $Li[Li_{1/3}Ti_{5/3}]O_4$ and $Li_{1/2}Fe_{1/2}[Li_{1/2}Fe_{1/2}Ti]O_4$ was carried out in order to understand zero-strain insertion mechanism. Degree of defect defined by the occupation of lithium ions at 16(d) sites in $Fd\bar{3}m$ is 0% in $Li[CrTi]O_4$, 17% in $Li[Li_{1/3}Ti_{5/3}]O_4$ and 25% in $Li_{1/2}Fe_{1/2}[Li_{1/2}Fe_{1/2}Ti]O_4$. Electrochemical tests in non-aqueous lithium cells indicated that no fatal damage was observed with respect to XRD even for 25% defect of spinel-framework structure based on lithium titanium oxides. All samples examined here show the character of so-called zero-strain lithium insertion materials while $Li_{1/2}Fe_{1/2}[Li_{1/2}Fe_{1/2}Ti]O_4$ is converted to a rock-salt structure of $Li_{3/2}Fe_{1/2}[Li_{1/2}Fe_{1/2}Ti]O_4$ in which Fe^{3+} ions at the tetrahedral sites move to the octahedral sites by changing oxidation state on reduction. FT-IR and Raman spectral measurements were also carried out and the factors affecting zero-strain insertion mechanism were discussed.

Keywords: Lithium-ion battery; Zero-strain insertion materials; Lithium titanium oxides; Topotactic reaction

1. Introduction

Zero-strain insertion material is an ideal electrode for long-life lithium-ion batteries. Such a material reported so far is $Li[Li_{1/3}Ti_{5/3}]O_4$ in spite of extensive search for new materials for advanced lithium-ion batteries. $Li[Li_{1/3}Ti_{5/3}]O_4$ shows extremely flat operating voltage of 1.55 V against a lithium electrode with rechargeable capacity of 170 mAh g^{-1}, so that this is a negative-electrode material for lithium-ion batteries [1]. In order to understand zero-strain mechanism and then to explore zero-strain insertion material for positive electrode, a series of experimental and theoretical works are undertaken.

In this paper, we prepare three samples, i.e. $Li[CrTi]O_4$, $Li[Li_{1/3}Ti_{5/3}]O_4$ and $Li_{1/2}Fe_{1/2}[Li_{1/2}Fe_{1/2}Ti]O_4$, having spinel-framework structure and examine lithium insertion schemes, and we discuss as to what key factors are for materials to be zero-strain and whether or not we can design zero-strain insertion material for positive electrode in lithium-ion batteries.

2. Experimental

$Li[CrTi]O_4$, $Li[Li_{1/3}Ti_{5/3}]O_4$ and $Li_{1/2}Fe_{1/2}[Li_{1/2}Fe_{1/2}Ti]O_4$ were prepared by solid-state reaction as were described previously [1–3]. The samples were characterized by X-ray diffraction (XRD), Fourier-transform infrared (FT-IR) and Raman spectroscopy. XRD data were obtained by using X-ray diffractometer (Type XD-3A, Shimadzu Corp., Ltd.) with Cu Kα radiation, equipped with diffracted beam graphite monochromator. FT-IR spectra were recorded by a KBr method using a FT-IR spectrometer 8300 (Shimadzu Corp., Ltd.). Raman spectra were obtained by using Raman microscopy system 'LabRam' (Horiba Corp., Ltd.). The excitation wavelength was 514 nm supplied by an Ar laser (0.6–6 mW). The laser beam was focused on the area of about 3 μmΦ.

For electrochemical tests, the electrodes were prepared by casting a slurry of 88 weight percent (wt.%) active materials, 6 wt.% acetylene black and 6 wt.% PVdF dispersed in *N*-methl-2-pyrrolidone (NMP) on an aluminum foil. NMP was evaporated at 60 °C for 30 min under vacuum, and finally the electrodes (15 mm × 20 mm) were dried under vacuum

* Corresponding author.
E-mail address: ohzuku@a-chem.eng.osaka-cu.ac.jp (T. Ohzuku).

0378-7753/$ – see front matter © 2005 Elsevier B.V. All rights reserved.
doi:10.1016/j.jpowsour.2005.03.019

at 150 °C for 12 h. Lithium metal was used as a negative electrode (15 mm × 20 mm). Two sheets of polypropylene porous membrane (Celgard2500) were used as a separator. Electrolyte used was 1 M $LiPF_6$ dissolved in ethylene carbonate (EC)/dimethyl carbonate (DMC) (3/7 v/v) solution. In fabricating cells, all materials except the electrolyte and lithium metal were dried under vacuum at 60 °C for at least 2 h to avoid possible contamination of water. All procedures for handling and fabricating the electrochemical cells were performed in an argon-filled glove box.

3. Results and discussion

Fig. 1 shows the XRD patterns of (a) $Li[CrTi]O_4$, (b) $Li[Li_{1/3}Ti_{5/3}]O_4$ and (c) $Li_{1/2}Fe_{1/2}[Li_{1/2}Fe_{1/2}Ti]O_4$. Miller indexes are given by assuming a space group of $Fd\bar{3}m$ [1]. Lattice parameters were calculated to be (a) 8.32, (b) 8.36 and (c) 8.36 Å. For a normal spinel $Li[B_2]O_4$ having a space group symmetry of $Fd\bar{3}m$, Li is located at the tetrahedral 8(a) sites and B (Ti, V, Mn or Ni) is located at the octahedral 16(d) sites in a cubic close-packed oxygen array. In performing topotactic electrochemical reactions of lithium transition metal oxides, we need tough matrixes against solid-state redox reactions of transition metal ions together with lithium ion insertion and/or extraction. Tough matrix was believed to be formed by octahedral linkage based on transition metal ions at the 16(d) sites surrounding by six oxygen ions, called spinel-framework structures. In other words, defect is not allowed at the 16(d) sites to form a tough matrix with which we have explained solid-state electrochemical reactions of $Li[B_2]O_4/Li_2[B_2]O_4$ or $\square[B_2]O_4/Li[B_2]O_4$ without the destruction of core structures in an early stage of our investigation [4]. However, lithium insertion materials of $Li[Li_xMn_{2-x}]O_4$ and $Li[Li_{1/3}Ti_{5/3}]O_4$ cannot be explained by such an ideal model on a spinel-framework structure. No selective line broadening was found in XRD for a series of $Li[Li_xMn_{2-x}]O_4$ and $Li[Li_{1/3}Ti_{5/3}]O_4$ samples [1,5]. Such a situation is better illustrated in Fig. 1. In $Li[CrTi]O_4$, the 16(d) sites are 100% occupied by transition metal ions (50% Cr^{3+} and 50% Ti^{4+}). In $Li[Li_{1/3}Ti_{5/3}]O_4$, 17% of titanium ions situated at the 16(d) sites are replaced by lithium ions. If cation ordering of Ti^{4+} and Li^+ existed in $Li[Li_{1/3}Ti_{5/3}]O_4$, XRD can be detected because of the difference in atomic scattering factors between Ti^{4+} and Li^+. If not, tough matrix or highly-crystallized material cannot be expected because covalency between Ti^{4+}–O^{2-} and Li^+–O^{2-} is intuitively different, which may result in ill-defined diffraction lines or at least selected line broadening in XRD. However, we cannot see any selective line broadening. As can be seen in Fig. 1, $Li[Li_{1/3}Ti_{5/3}]O_4$ is crystallized as high as that comparative to $Li[CrTi]O_4$. In $Li_{1/2}Fe_{1/2}[Li_{1/2}Fe_{1/2}Ti]O_4$, 25% of the 16(d) sites are occupied by lithium ions and Fe^{3+} (high spin state) is distributed in tetrahedral 8(a) and octahedral 16(d) sites, so that this is one of inverse-spinels. If we assume high-spin state of Fe^{3+} (d^5; ^6S) is equivalent to Li^+ (^0S) with respect to structural inorganic chemistry of $LiFeO_2$, 50% of titanium ions at the 16(d) sites are missing in $Li_{1/2}Fe_{1/2}[Li_{1/2}Fe_{1/2}Ti]O_4$. Even when 50% of defect stated above, well-defined diffraction lines are observed.

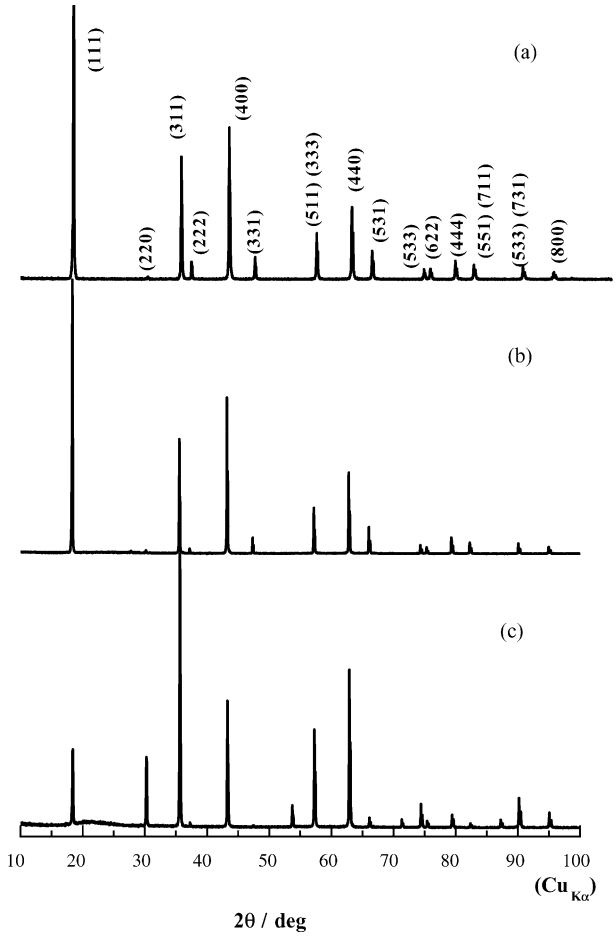

Fig. 1. XRD patterns of (a) $Li[CrTi]O_4$ (a = 8.32 Å), (b) $Li[Li_{1/3}Ti_{5/3}]O_4$ (a = 8.36 Å) and (c) $Li_{1/2}Fe_{1/2}[Li_{1/2}Fe_{1/2}Ti]O_4$ (a = 8.36 Å). Degree of defect defined by occupation of lithium ions at 16(d) sites in $Fd\bar{3}m$ is 0% in $Li[CrTi]O_4$, 17% in $Li[Li_{1/3}Ti_{5/3}]O_4$ and 25% in $Li_{1/2}Fe_{1/2}[Li_{1/2}Fe_{1/2}Ti]O_4$.

Fig. 2 shows the FT-IR and Raman spectra of (a) $Li[CrTi]O_4$, (b) $Li[Li_{1/3}Ti_{5/3}]O_4$ and (c) $Li_{1/2}Fe_{1/2}[Li_{1/2}Fe_{1/2}Ti]O_4$. According to factor group analysis [6], four IR-active modes ($4F_{1u}$) and five Raman-active modes ($A_{1g} + E_g + 3F_{2g}$) are expected for a normal spinel (O_h^7). Among Raman spectra in Fig. 2, Raman spectrum of $Li[Li_{1/3}Ti_{5/3}]O_4$ is anomalous because more than five Raman lines are observed, i.e. at least eight vibration modes. If the space group symmetry to describe crystal structure of $Li[Li_{1/3}Ti_{5/3}]O_4$ reflect on number of Raman lines, symmetry is lower than $Fd\bar{3}m$ as were seen for $Li[Ni_{1/2}Mn_{3/2}]O_4$ [7].

Fig. 3 shows the charge and discharge curves of lithium cells of (a) $Li[CrTi]O_4$, (b) $Li[Li_{1/3}Ti_{5/3}]O_4$ and (c) $Li_{1/2}Fe_{1/2}[Li_{1/2}Fe_{1/2}Ti]O_4$. Cells were operated at a rate of 0.17 mA cm^{-2} in voltage of 1.0–3.0 V at 30 °C. $Li[CrTi]O_4$ and $Li[Li_{1/3}Ti_{5/3}]O_4$ show extremely flat operating

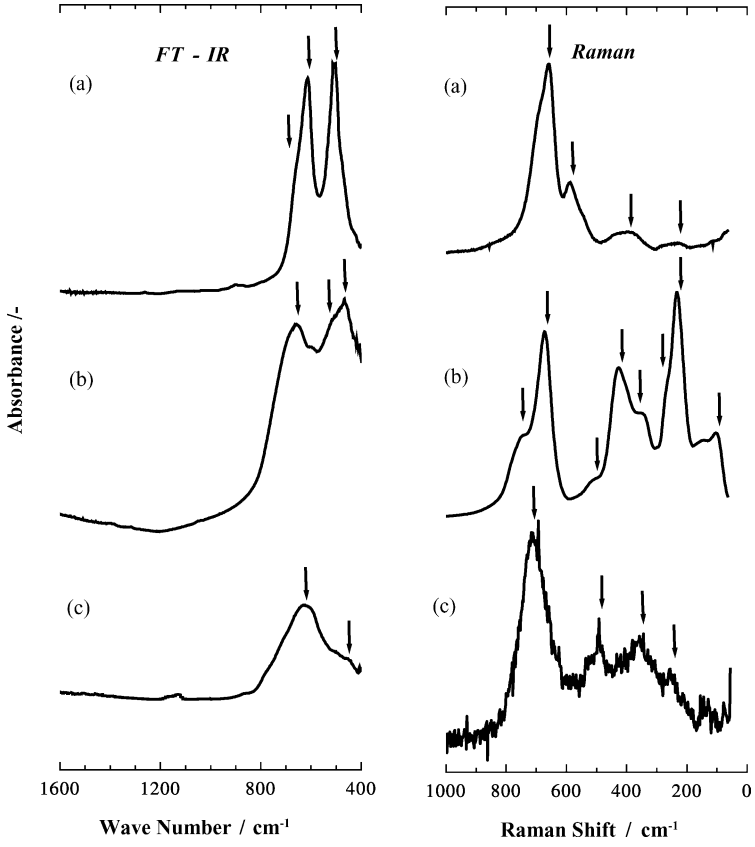

Fig. 2. FT-IR (left) and Raman (right) spectra of (a) $Li[CrTi]O_4$, (b) $Li[Li_{1/3}Ti_{5/3}]O_4$ and (c) $Li_{1/2}Fe_{1/2}[Li_{1/2}Fe_{1/2}Ti]O_4$. Active vibration modes for $Fd\bar{3}m$ (O_h^7) are estimated to be four vibration modes ($4F_{1u}$) for IR and five vibration modes ($A_{1g} + E_g + 3F_{2g}$) for Raman, respectively, from factor group analysis [6].

voltage of about 1.5 V against a lithium electrode. Rechargeable capacities are ca. 95% of theoretical capacities. Since $Li_{1/2}Fe_{1/2}[Li_{1/2}Fe_{1/2}Ti]O_4$ is one of the inverse-spinel structures, electrochemical reactivity is not expected in a topotactic manner because Fe^{3+} ions at the 8(a) sites block lithium-ion diffusion and migration throughout a solid matrix. However, fact is that ca. 120 mAh g^{-1} rechargeable capacity based on $Li_{1/2}Fe_{1/2}[Li_{1/2}Fe_{1/2}Ti]O_4$ sample weight was observed. Capacity of 120 mAh g^{-1} corresponds to about 80% of utilization based on 153 mAh g^{-1} of theoretical capacity, assuming one-electron transfer. Cycleability is poor compared to $Li[CrTi]O_4$ or $Li[Li_{1/3}Ti_{5/3}]O_4$. Operating voltage is above 2 V, which is 0.6 V higher than that for $Li[CrTi]O_4$ or $Li[Li_{1/3}Ti_{5/3}]O_4$.

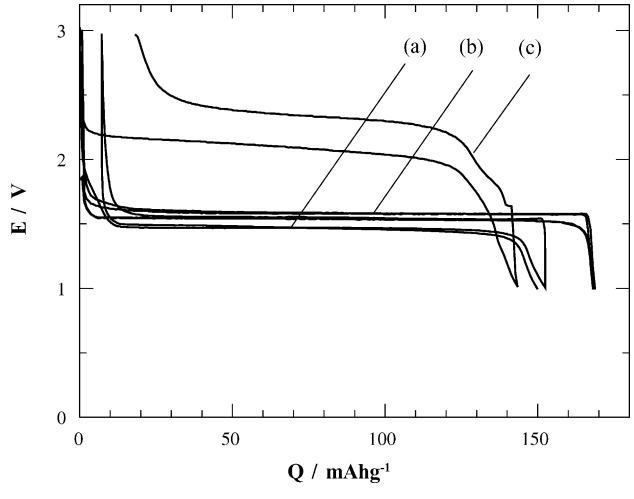

Fig. 3. Charge and discharge curves of lithium cells of (a) $Li[CrTi]O_4$, (b) $Li[Li_{1/3}Ti_{5/3}]O_4$ and (c) $Li_{1/2}Fe_{1/2}[Li_{1/2}Fe_{1/2}Ti]O_4$. Cells were operated at a rate of 0.17 mA cm^{-2} in voltage of 1.0–3.0 V at 30 °C.

Fig. 4 shows the XRD patterns of the reduced forms of (a) $Li[CrTi]O_4$ (155 mAh g^{-1} of the degree of reduction), (b) $Li[Li_{1/3}Ti_{5/3}]O_4$ (160 mAh g^{-1}) and (c) $Li_{1/2}Fe_{1/2}[Li_{1/2}Fe_{1/2}Ti]O_4$ (140 mAh g^{-1}). As can be seen in Figs. 1 and 4, $Li[CrTi]O_4$ expands its cubic lattice from $a = 8.32$ to 8.34 Å while $Li[Li_{1/3}Ti_{5/3}]O_4$ does not change in its cubic lattice ($a = 8.36$ Å) on discharge in non-aqueous lithium cells. Striking feature can be seen in Fig. 1(c) and Fig. 4(c) for $Li_{1/2}Fe_{1/2}[Li_{1/2}Fe_{1/2}Ti]O_4$. In Fig. 1(c) for starting material of $Li_{1/2}Fe_{1/2}[Li_{1/2}Fe_{1/2}Ti]O_4$ (3 1 1) line is the strongest among 16 diffraction lines and (2 2 0) line is clearly seen. In reduced form of $Li_{1/2}Fe_{1/2}[Li_{1/2}Fe_{1/2}Ti]O_4$ shown in Fig. 4(c) (4 0 0) line is the strongest among eight diffraction lines observed. (3 1 1) and (2 2 0) lines are reduced in their intensities for the reduced form. This can be explained by assuming that one of the inverse-spinel

Table 1
Change in unit cell volume for lithium titanium oxides

Materials	Unit cell volume of pristine material (Å^3)	Unit cell volume in discharged state (Å^3)	Change in volume ΔV (%)
$Li[CrTi]O_4$	576	580	+0.7
$Li[Li_{1/3}Ti_{5/3}]O_4$	585	585	0.0
$Li_{1/2}Fe_{1/2}[Li_{1/2}Fe_{1/2}Ti]O_4$	584	587	+0.4
$LiTi_2O_4$ [8]	593	587	−1.0
TiO_2 (anatase) [9]	136	141	+3.7

$Li_{1/2}Fe_{1/2}[Li_{1/2}Fe_{1/2}Ti]O_4$ is transformed to rock-salt structure $Li_{3/2}Fe_{1/2}[Li_{1/2}Fe_{1/2}Ti]O_4$ in which all cations are located at the octahedral sites. Although change in XRD patterns is destructive, this process is reversible in limited cycles. Cubic lattice parameter in Fig. 4(c) is calculated to be 8.37 Å, which is almost the same as 8.36 Å in Fig. 1(c). Selective line broadening is not observed even in reduced form of $Li_{1/2}Fe_{1/2}[Li_{1/2}Fe_{1/2}Ti]O_4$. As far as change in lattice dimensions is concerned, lithium-ion titanium oxide ($Fd\bar{3}m$) is one of the so-called zero-strain insertion electrodes although zero-strain mechanism is derived from the reversible movements of iron species in cubic close-packed oxygen array.

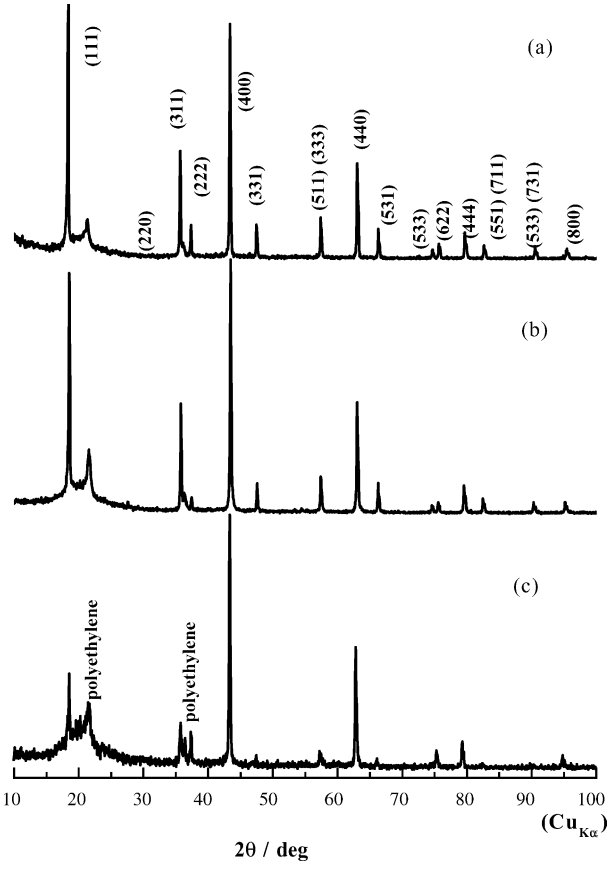

Fig. 4. XRD patterns of (a) $Li_2[CrTi]O_4$ (a = 8.34 Å), (b) $Li_2[Li_{1/3}Ti_{5/3}]O_4$ (a = 8.36 Å) and (c) Li_2FeTiO_4 (a = 8.37 Å). All samples were prepared by electrochemical reduction in non-aqueous lithium cells. The discharge capacities of each sample are 155 mAh g^{-1} for (a) $Li_2[CrTi]O_4$; 160 mAh g^{-1}, (b) $Li_2[Li_{1/3}Ti_{5/3}]O_4$; 140 mAh g^{-1} and (c) Li_2FeTiO_4.

Table 1 summarized the change in lattice volume for lithium titanium oxides. $LiTi_2O_4$ [8] and TiO_2 (anatase) [9] are also given in Table 1. Maximum volume change among these samples is observed from TiO_2 (anatase; $I4_1/amd$), which is not cubic symmetry. As seen in Table 1, lithium titanium oxides with or without defect having space group symmetry of $Fd\bar{3}m$ show small change in lattice volume, below 1%. When lithium ions and electrons are inserted into a solid matrix (reduction of material), lattice dimension usually expands mainly due to the reduction of transition metal ions (expansion of ionic size). For $LiTi_2O_4$ in Table 1, lattice volume is reduced by 1% when $LiTi_2O_4$ is electrochemically reduced to $Li_2Ti_2O_4$.

As were described above, cubic close-packed oxygen array, defect of transition metal ions at 16(d) sites in $Fd\bar{3}m$, and mobile cations are keys to understand zero-strain insertion mechanism of $Li[Li_{1/3}Ti_{5/3}]O_4$. The first-principles calculation combined with HRTEM and SAED observations will give more insights into zero-strain insertion materials. Such an approach is now in progress in our research groups.

Acknowledgements

One of us (K.M.) wishes to thank Dr. Yoshio Ukyo of TCRDL for giving him a chance to attend OCU research group in academic years of 2001–2002. The present work was partially supported by a grant-in-aid from the Osaka City University (OCU) Science Foundation.

References

[1] T. Ohzuku, A. Ueda, N. Yamamoto, J. Electrochem. Soc. 142 (1995) 1431.
[2] T. Ohzuku, K. Tatsumi, N. Matoba, K. Sawai, J. Electrochem. Soc. 147 (2000) 3592.
[3] T. Ohzuku, K. Tatsumi, K. Ariyoshi, Proceedings of the 40th Battery Symposium, Kyoto, 1999 (abstract no. 2C06).
[4] T. Ohzuku, M. Kitagawa, T. Hirai, J. Electrochem. Soc. 137 (1990) 769.
[5] T. Ohzuku, S. Kitanno, M. Iwanaga, H. Matsuno, A. Ueda, J. Power Sources 68 (1997) 646.
[6] S. Bhagavantam, T. Venkatarayudu, Theory of Groups and its Application to Physical Problems, Academic Press, 1969, p. 140.
[7] K. Ariyoshi, Y. Iwakoshi, N. Nakayama, T. Ohzuku, J. Electrochem. Soc. 15 (2004) A296.
[8] K.M. Colbow, J.R. Dahn, R.R. Haering, J. Power Sources 26 (1989) 397.
[9] T. Ohzuku, T. Kodama, T. Hirai, J. Power Sources 14 (1985) 153.